Characterization of $NiSO_4$ Supported on Fe_2O_3 and Catalytic Properties for Ethylene Dimerization

Young Il Pae[†] and Jong Rack Sohn[*]

Department of Applied Chemistry, Engineering College, Kyungpook National University, Daegu 702-701, Korea
[*]E-mail: jrsohn@knu.ac.kr
[†]Department of Chemistry, University of Ulsan, Ulsan 680-746, Korea
Received May 22, 2007

The $NiSO_4$ supported on Fe_2O_3 catalysts were prepared by the impregnation method. No diffraction line of nickel sulfate was observed up to 30 wt %, indicating good dispersion of nickel sulfate on the surface of Fe_2O_3. The addition of nickel sulfate to Fe_2O_3 shifted the phase transition of Fe_2O_3 (from amorphous to hematite) to higher temperatures because of the interaction between nickel sulfate and Fe_2O_3. 20-$NiSO_4/Fe_2O_3$ containing 20 wt % of $NiSO_4$ and calcined at 500 °C exhibited a maximum catalytic activity for ethylene dimerization. The initial product of ethylene dimerization was found to be 1-butene and the initially produced 1-butene was also isomerized to 2-butene during the reaction. The catalytic activities were correlated with the acidity of catalysts measured by the ammonia chemisorption method.

Key Words : $NiSO_4/Fe_2O_3$ catalyst, Phase transition of Fe_2O_3, Acidic properties, Ethylene dimerization

Introduction

Heterogeneous catalysts for the dimerization and oligomerization of olefins, consisting mainly of nickel compounds supported on oxides, have been known for many years. The dimerization of alkenes is an important method for the production of higher olefins which find extensive application as industrial intermediate. A considerable number of papers have dealt with the problem of nickel-containing catalysts for ethylene dimerization.[1-11] One of the remarkable features of this catalyst system is its activity in relation to a series of *n*-olefins. In contrast to usual acid-type catalysts, nickel oxide on silica or silica-alumina shows a higher activity for a lower olefin dimerization, particularly for ethylene.[1-6,12] It has been suggested that the active site for dimerization is formed by an interaction of a low-valent nickel ion with an acid site.[9,13] It has been reported that the dimerization activities of such catalysts are related to the acidic properties of surface and low valent nickel ions. In fact, nickel oxide, which is active for C_2H_4-C_2D_4 equilibration, acquires an activity for ethylene dimerization upon addition of nickel sulfate, which is known to be an acid[14] A transition metal can also be supported on zeolite in the state of a cation or a finely dispersed metal. Transition metal ions like Ni^+ or Pd^+ can be active sites in catalytic reactions such as ethylene and propylene dimerization as well as acetylene cyclomerization.[15-17]

Many metal sulfates generate fairly large amounts of acid sites of moderate or strong strength on their surfaces when they are calcined at 400-700 °C.[18,19] The acidic property of metal sulfate often gives high selectivity for diversified reactions such as hydration, polymerization, alkylation, cracking, and isomerization. However, structural and physicochemical properties of supported metal sulfates are considered to be in different states compared with bulk metal sulfates because of their interaction with supports[9,10,20] In the case of sulfate-promoted Fe_2O_3, the gas-phase skeletal isomerization of n-butane to isobutene took place even at 25 °C.[21] From this fact, Fe_2O_3/SO_4^{2-} was regarded as a superacid. This catalyst also showed high catalytic activities for the polymerization of alkyl vinyl ether,[22] the double bond isomerization isomerization of 1-butene,[23] the ring-opening isomerization of cyclopropane,[23,24] the dehydration of 2-butanol,[23,24] and the liquefaction of coal.[25] Sulfated zirconia incorporating Fe and Mn has been shown to be highly active for butane isomerization, catalyzing the reaction even at room temperature.[26,27] Coelho *et al.* have discovered that the addition of Ni to sulfated zirconia causes an activity enhancement comparable to that caused the addition of Fe and Mn.[28]

So far, however, supported nickel sulfate catalysts have been used mainly on alumina, zirconia, and titania-zirconia.[1,9,29,30] $NiSO_4$ catalyst supported on Fe_2O_3 for ethylene dimerization have not been reported up to now. Therefore, in this paper, we tried to prepare new catalyst systems by supporting $NiSO_4$ on Fe_2O_3. Characterization of $NiSO_4/Fe_2O_3$ and catalytic activity for ethylene dimerization are reported.

Experimental Section

Catalyst preparation. The catalysts was prepared as follows. The precipitate of $Fe(OH)_3$ was obtained by adding aqueous ammonia slowly into an aqueous solution of iron nitrate at room temperature with stirring until the pH of the mother liquor reached about 8. The precipitate, thus, obtained was washed thoroughly with distilled water and was dried at 100 °C. The precipitate powdered below 100 mesh. Catalysts containing various nickel sulfate contents were prepared by the impregnation of $Fe(OH)_3$ powder with

an aqueous solution of $NiSO_4$, followed by calcining at different temperatures for 1.5 h in air. This series of catalysts is denoted by the weight percentage of nickel sulfate. For example, 20-$NiSO_4/Fe_2O_3$ indicates the catalyst containing 20 wt % of $NiSO_4$.

Procedure. FTIR spectra were obtained in a heatable gas cell at room temperature using a Mattson Model GL6030E spectrophotometer. The self-supporting catalyst wafers contained about 10 mg cm^{-2}. Prior to obtaining the spectra, we heated each sample under vacuum at 25-500 °C for 1 h. Catalysts were checked in order to determine the structure of the prepared catalysts by means of a Philips X'pert-APD X-ray diffractometer, employing Ni-filtered Cu K_α radiation. DSC measurements were performed by a PL-STA model 1500H apparatus in air; the heating rate was 5 °C per min. For each experiment 10-15 mg of sample was used.

The specific surface area was determined by applying the BET method to the adsorption of N_2 at −196 °C. Chemisorption of ammonia was also employed as a measure of the acidity of catalysts. The amount of chemisorption was determined based on the irreversible adsorption of ammonia.[31,32]

The catalytic activity for ethylene dimerization was determined at 20 °C using a conventional static system following the pressure change from an initial pressure of 290 Torr. A fresh catalyst sample of 0.2 g was used for every run and the catalytic activity was calculated as the number of moles of ethylene. Reaction products were analyzed by gas chromatography with a VZ-7 column at room temperature.

Results and Discussion

Infrared spectra. The infrared spectra of 20-$NiSO_4/Fe_2O_3$ (KBr disc) calcined at different temperatures (300-800 °C) are given in Figure 1. 20-$NiSO_4/Fe_2O_3$ calcined up to 700 °C showed infrared absorption bands at 1201, 1133, 1098 and 987 cm^{-1}, which are assigned to bidentate sulfate ions coordinated to the metal, such as Fe^{3+} or Ni^{2+}.[31,32] For 20-$NiSO_4/Fe_2O_3$ calcined at 700 °C, the band intensities of sulfate ion decreased because of the partial decomposition of sulfate ion. However, for the sample calcined at 800 °C, infrared bands by the sulfate ion disappeared completely due to the decomposition of sulfate ion.

In general, for the metal oxides modified with sulfate ions followed by evacuation above 400 °C, a strong band[33,34] assigned to S=O stretching frequency is observed at 1390-1360 cm^{-1}. In a separate experiment, the infrared spectrum of self-supported 20-$NiSO_4/Fe_2O_3$ after evacuation at 500 °C for 1 h was examined. As shown in Figure 1, there is an intense band at 1376 cm^{-1}, accompanied by four broad but split bands at 1182, 1133, 1028 and 970 cm^{-1}, indicating the presence of different adsorbed species depending on the treatment conditions of the sulfated sample.[35]

Crystalline structures of catalysts. The crystalline structures of Fe_2O_3 calcined in air at different temperatures for 1.5 h were checked by X-ray diffraction. As shown in Figure 2, Fe_2O_3 was amorphous to X-ray diffraction at 25 °C. However, from 300 °C the phase transition of Fe_2O_3 from amorphous to hematite occurred, showing that the intensity of hematite increased with the calcination temperature. In the case of supported nickel sulfate catalysts, the crystalline structures of the samples were different from that of the Fe_2O_3 support. The 20-$NiSO_4/Fe_2O_3$ materials calcin-

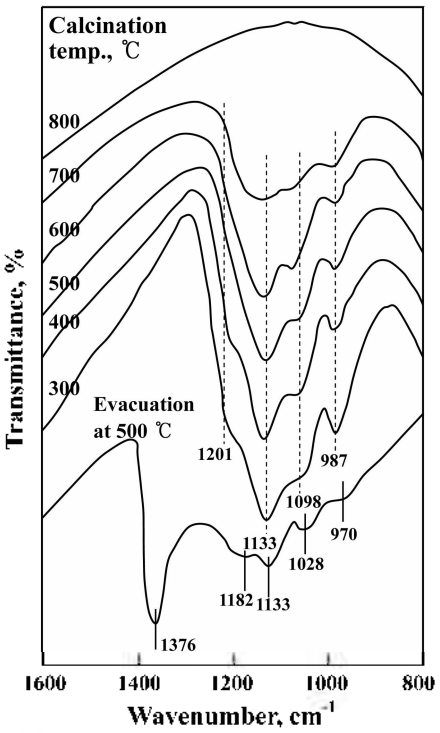

Figure 1. Infrared spectra of 20-$NiSO_4/Fe_2O_3$ calcined at different temperatures for 1.5 h.

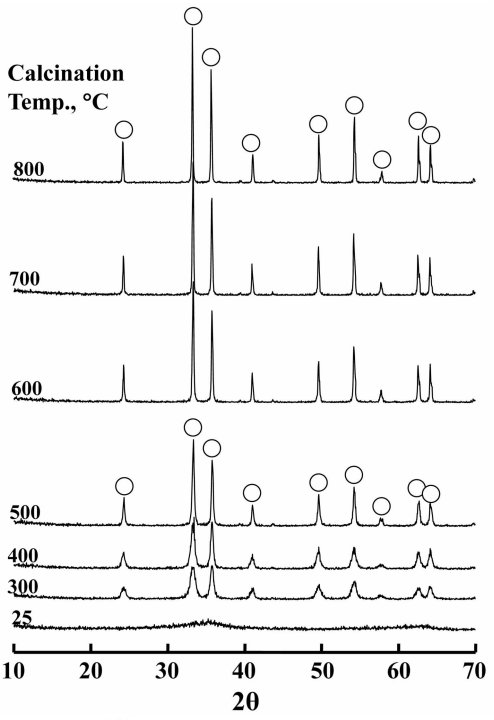

Figure 2. X-ray diffraction patterns of Fe_2O_3 calcined at different temperatures for 1.5 h : (○), hematite phase of Fe_2O_3.

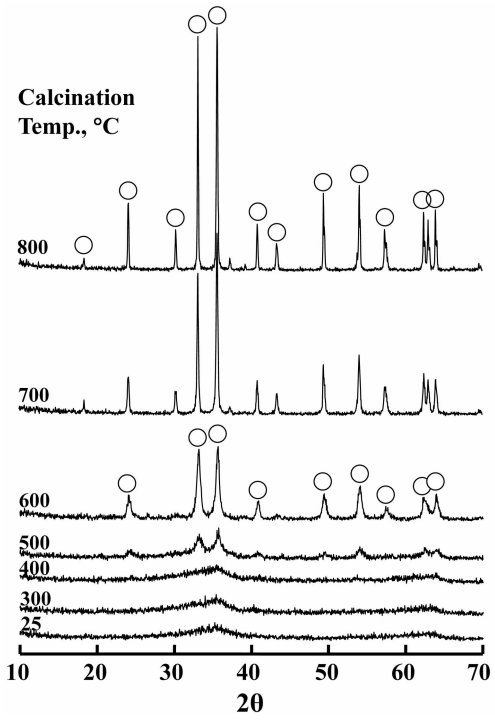

Figure 3. X-ray diffraction patterns of 20-$NiSO_4/Fe_2O_3$ calcined at different temperatures for 1.5 h: (○), hematite phase of Fe_2O_3.

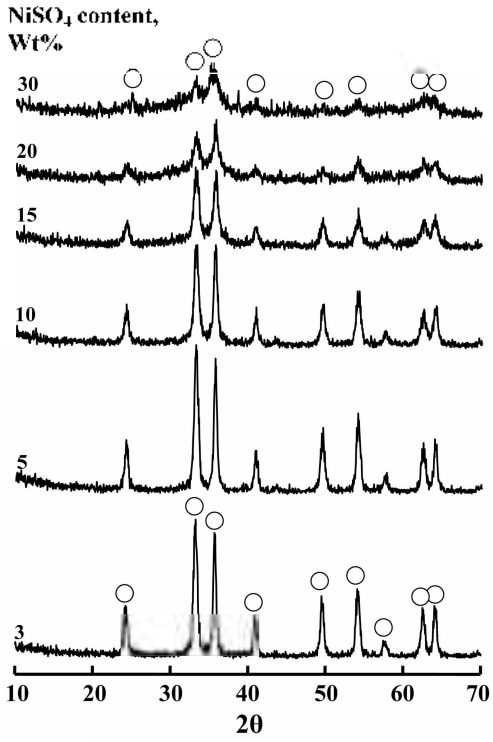

Figure 4. X-ray diffraction patterns of $NiSO_4/Fe_2O_3$ containing different $NiSO_4$ contents and calcined at 500 °C for 1.5 h: (○), hematite phase of Fe_2O_3.

ed at different temperatures, as shown in Figure 3, are amorphous up to 400 °C. In other words, the transition temperature from amorphous to hematite phase was higher by 200 °C than that of pure Fe_2O_3.[36] These results are similar to those of supported ZrO_2 catalysts, where the transition temperature from amorphous to tetragonal ZrO_2 phase was higher by 200 °C than that of pure ZrO_2.[36] X-ray diffraction data indicated only the hematite phase of Fe_2O_3 at 500-800 °C, without detection of orthorhombic $NiSO_4$ phase. It is assumed that the interaction between $NiSO_4$ and Fe_2O_3 hinders the phase transition of Fe_2O_3 from amorphous to hematite.[37] In this case, the amount of hematite also increased with the calcination temperature.

The XRD patterns of $NiSO_4/Fe_2O_3$ containing different nickel sulfate contents and calcined at 500 °C for 1.5 h are shown in Figure 4. XRD data indicated only hematite phase of Fe_2O_3 at the region of 3-30 wt % of nickel sulfate, indicating good dispersion of $NiSO_4$ on the surface of Fe_2O_3. However, the higher the content of $NiSO_4$, the lower is the amount of hematite Fe_2O_3 phase, because the interaction between nickel sulfate and Fe_2O_3 hinders the phase transition of Fe_2O_3 from amorphous to hematite in proportion to the nickel sulfate content.[32]

Thermal analysis. The X-ray diffraction patterns in Figures 2-4 clearly show that the structure of $NiSO_4/Fe_2O_3$ is different depending on the calcined temperature. To examine the thermal properties of precursors of $NiSO_4/Fe_2O_3$ samples more clearly, we completed their thermal analysis; the results are illustrated in Figure 5. For pure Fe_2O_3, the DSC curve shows a broad endothermic peak below 200 °C due to water elimination, and an exothermic peak at 351 °C due to

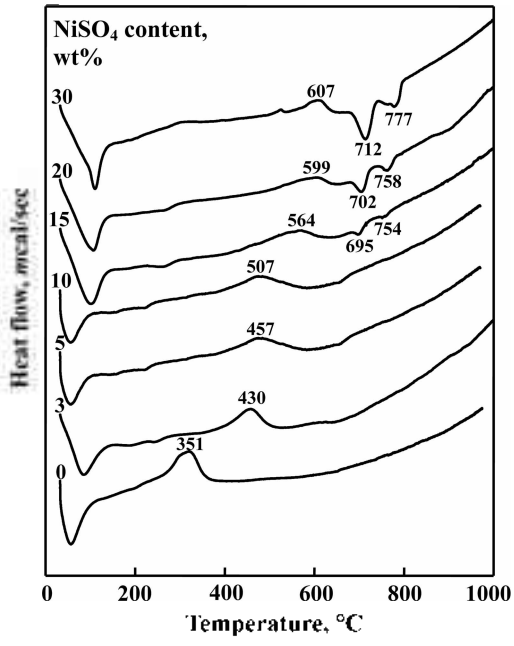

Figure 5. DSC curves of $NiSO_4/Fe_2O_3$ precursors containing different $NiSO_4$ contents.

the Fe_2O_3 crystallization from amorphous to hematite phase.[32] However, it is of interest to see the influence of $NiSO_4$ on the crystallization of Fe_2O_3 from amorphous to hematite phase. As Figure 5 shows, the exothermic peak due to the crystallization appears at 351 °C for pure Fe_2O_3, while for $NiSO_4/Fe_2O_3$ samples it is shifted to higher temperatures

due to the interaction between $NiSO_4$ and Fe_2O_3. The shift increases with increasing $NiSO_4$ content. Consequently, the exothermic peaks appear at 430 °C for 3-$NiSO_4/Fe_2O_3$, 457 °C for 5-$NiSO_4/Fe_2O_3$, 507 °C for 10-$NiSO_4/Fe_2O_3$, 564 °C for 15-$NiSO_4/Fe_2O_3$, 599 °C for 20-$NiSO_4/Fe_2O_3$, and 607 °C for 30-$NiSO_4/Fe_2O_3$.

The endothermic peaks for $NiSO_4/Fe_2O_3$ samples containing $NiSO_4$ content above 10 wt % in the region of 700-777 °C are due to the evolution of SO_3 decomposed from sulfate species bonded to the surface of Fe_2O_3. However, as shown in Figure 5, two endothermic peaks for some samples due to the evolution of SO_3 indicate that there are two different sulfate species on the surface of catalyst. For pure $NiSO_4 \cdot 6H_2O$, the DSC curve shows three endothermic peaks below 400 °C due to water elimination, indicating that the dehydration of $NiSO_4 \cdot 6H_2O$ occurs in three steps. The endothermic peak around 837 °C is due to the evolution of SO_3 decomposed from nickel sulfate.[37,38] Decomposition of nickel sulfate is known to begin at 700 °C.[39]

Specific surface area and acidity. The specific surface areas of samples containing different $NiSO_4$ contents and calcined at 500 °C for 1.5 h are listed in Table 1. The presence of nickel sulfate influences the surface area in comparison with that of the pure Fe_2O_3. Specific surface areas of $NiSO_4/Fe_2O_3$ samples are larger than that of Fe_2O_3 calcined at the same temperature, showing that surface area increases gradually with increasing nickel sulfate loading up to 20 wt%. It seems likely that the interactions between nickel sulfate and Fe_2O_3 prevent catalysts from crystallizing.[40] The decrease of surface area for $NiSO_4/Fe_2O_3$ samples containing $NiSO_4$ above 20 wt % is due to the blocking of Fe_2O_3 pores by the increased $NiSO_4$ loading. The acidity of catalysts calcined at 500 °C, as determined by the amount of NH_3 irreversibly adsorbed at 230 °C,[31,32] is also listed in Table 1. The variation of acidity runs parallel to the change of surface area. The acidity increases with increasing nickel sulfate content up to 20 wt % of $NiSO_4$. The acidity is correlated with the catalytic activity for the ethylene dimerization discussed below. The surface area and acidity of 20-$NiSO_4/Fe_2O_3$ as a function of calcination temperature are listed in Table 2. Both surface area and acidity decreased with the calcination temperature. Also, in this case, the variation of acidity runs parallel to the change of surface area. Especially, the remarkable decrease of surface area and acidity after 600 °C of calcination temperature is due to the decomposition of sulfate species on the surface of 20-$NiSO_4/Fe_2O_3$, as shown in Figure 1.

Table 1. Surface area and acidity of $NiSO_4/Fe_2O_3$ catalysts containing different $NiSO_4$ contents and calcined at 500 °C for 1.5 h

$NiSO_4$ content (wt%)	Surface area (m^2/g)	Acidity (μmol/g)
0	10	21
3	20	121
5	44	138
10	51	153
15	63	240
20	75	304
30	56	278
100	30	79

Table 2. Surface area and acidity of 20-$NiSO_4/Fe_2O_3$ catalysts calcined at different temperatures for 1.5 h

Temperature (°C)	Surface area (m^2/g)	Acidity (μmol/g)
300	153	338
400	136	312
500	75	304
600	32	85
700	24	30
800	14	10

Infrared spectroscopic studies of ammonia adsorbed on solid surfaces have made it possible to distinguish between Brönsted and Lewis acid sites.[38,41,42] Figure 6 shows the infrared spectra of ammonia adsorbed on 20-$NiSO_4/Fe_2O_3$ samples evacuated at 500 °C for 1 h. For 20-$NiSO_4/Fe_2O_3$ the band at 1432 cm^{-1} is the characteristic peak of ammonium ion, which is formed on the Brönsted acid sites and the absorption peak at 1612 cm^{-1} is contributed by ammonia coordinately bonded to Lewis acid sites,[38,41,42] indicating the presence of both Brönsted and Lewis acid sites on the surface of 20-$NiSO_4/Fe_2O_3$ samples. Other samples having different nickel sulfate contents also showed the presence of both Lewis and Brönsted acids. As Figure 6(a) shows, the intense band at 1376 cm^{-1} after evacuation at 500 °C is assigned to the asymmetric stretching vibration of S=O bonds having a high double bond nature.[34,38] However, the drastic shift of the infrared band from 1376 cm^{-1} to a lower

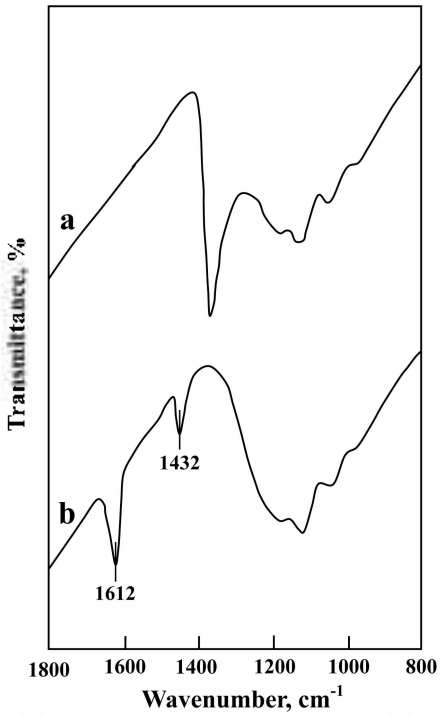

Figure 6. Infrared spectra of NH_3 adsorbed on 20-$NiSO_4/Fe_2O_3$: (a) background of 20-$NiSO_4/Fe_2O_3$ after evacuation at 500 °C for 1 h. (b) NH_3 adsorbed on (a), where gas was evacuated at 230 °C for 1 h.

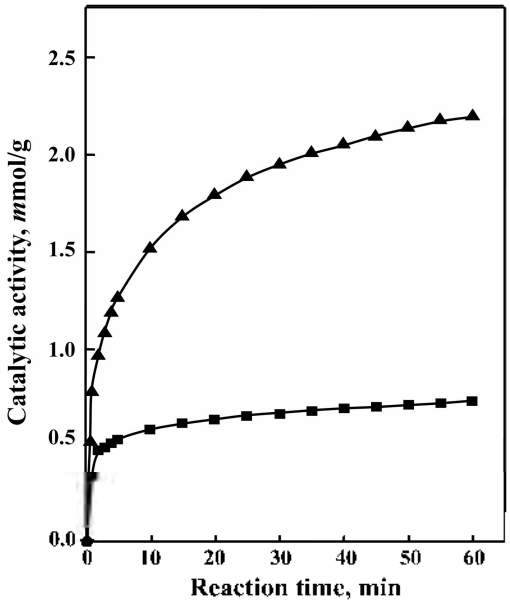

Figure 7. Time-course of ethylene dimerization over catalysts evacuated at 500 °C for 1 h: (▲), 20-$NiSO_4/Fe_2O_3$; (■) 5-$NiSO_4/Fe_2O_3$.

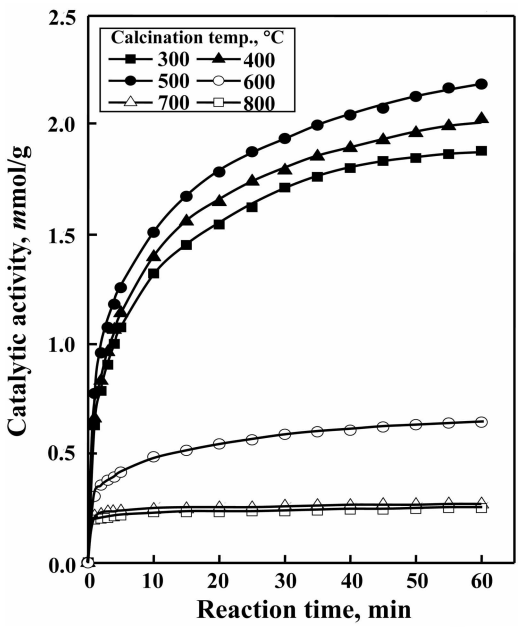

Figure 8. Catalytic activity of 20-$NiSO_4/Fe_2O_3$ for ethylene dimerization as a function of calcination temperature.

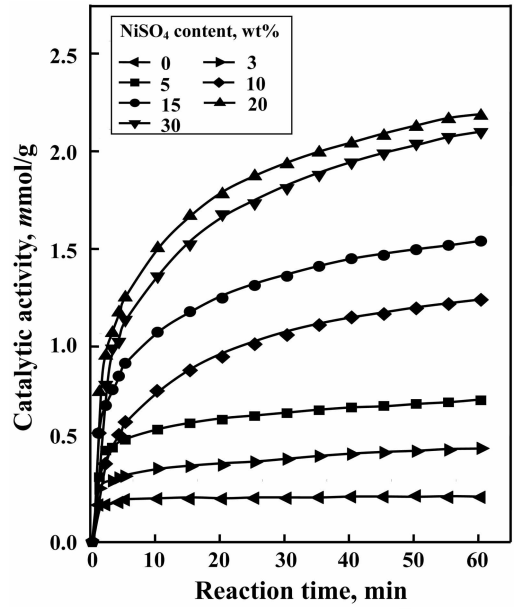

Figure 9. Catalytic activity of $NiSO_4/Fe_2O_3$ for ethylene dimerization as a function of $NiSO_4$ content.

wavenumber (not shown due to the overlaps of skeletal vibration bands of Fe_2O_3) after ammonia adsorption (Figure 6(b)) indicates a strong interaction between an adsorbed ammonia molecule and the surface complex. Namely, the surface sulfur compound in the highly acidic catalysts has a strong tendency to reduce the bond order of S=O from a highly covalent double-bond character to a lesser double-bond character when a basic ammonia molecule is adsorbed on the catalysts.[34,38]

Catalytic activities for ethylene dimerization. $NiSO_4/Fe_2O_3$ catalysts were tested for their effectiveness in ethylene dimerization. Over 5-$NiSO_4/FeO_3$ and 20-$NiSO_4/Fe_2O_3$, ethylene was continuously consumed, as shown by the results presented in Figure 7, where catalysts were evacuated at 500 °C for 1 h. Over two catalysts, ethylene was selectively dimerized to *n*-butenes. However, we detected a small amount of hexenes from the phase that had adsorbed on the catalyst surface. Therefore, the deactivation of catalyst occurred slowly due to the adsorption of oligomers. In the composition of *n*-butenes analyzed by gas chromatography, 1-butene was found to predominate exclusively at the initial reaction time, as compared with *cis*-butene and *trans*-butene. This is because the initial product of ethylene dimerization is 1-butene.[4,9,42] Therefore, the initially produced 1-butene is also isomerized to 2-butene during the reaction time.[38,43]

The catalytic activities of 20-$NiSO_4/Fe_2O_3$ were tested as a function of calcination temperature: the results are shown in Figure 8. The activities increased with the calcination temperature, reaching a maximum at 500 °C, and then the activities decreased. These results are very similar to those reported by other authors,[44,45] where sulfated Fe_2O_3 catalyst calcined at 500 °C exhibited a maximum catalytic activity. The decrease of catalytic activity after calcination above 500 °C can be probably attributed to the fact that the surface area and acidity above 500 °C decrease with the calcination temperature. As listed in Table 2, both surface area and acidity above 500 °C decreased with the calcination temperature.

Catalytic activity as a function of $NiSO_4$ content. The catalytic activity of $NiSO_4/Fe_2O_3$ containing different $NiSO_4$ contents was examined; the results are shown as a function of $NiSO_4$ content in Figure 9. Catalysts were evacuated at 500 °C for 1 h before each reaction. The catalytic activity gives a maximum at 20 wt % of $NiSO_4$. This seems to be

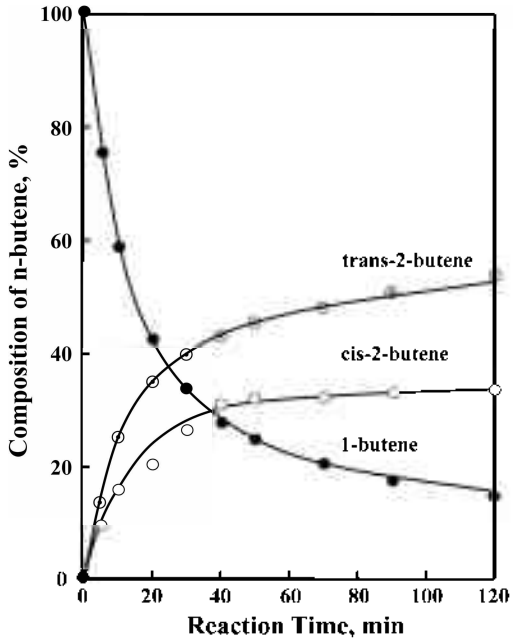

Figure 10. Variation of product composition in ethylene dimerization on 20-$NiSO_4/Fe_2O_3$ with reaction time.

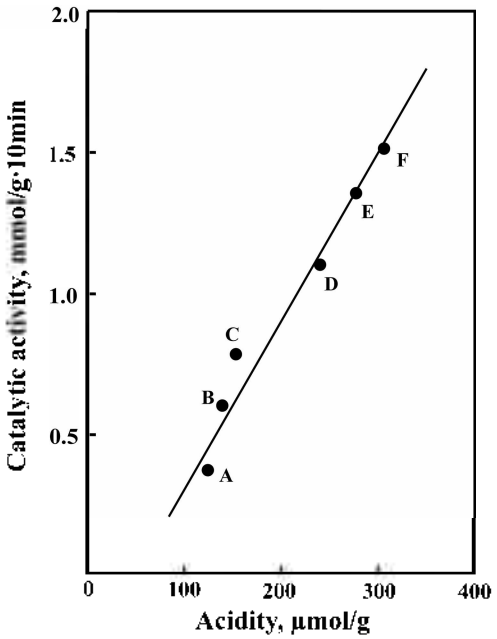

Figure 11. Correlationship between catalytic activity and acidity: (A) 3-$NiSO_4/Fe_2O_3$, (B) 5-$NiSO_4/Fe_2O_3$, (C) 10-$NiSO_4/Fe_2O_3$, (D) 15-$NiSO_4/Fe_2O_3$, (E) 30-$NiSO_4/Fe_2O_3$, and (F) 20-$NiSO_4/Fe_2O_3$.

correlated to the specific surface area and to the acidity of catalysts. The acidity of $NiSO_4/Fe_2O_3$ calcined at 500 °C was determined by the amount of NH_3 irreversibly adsorbed at 230 °C.[31,32] As listed in Table 1, the BET surface area attained a maximum extent when the $NiSO_4$ content in the catalyst was 20 wt % and then showed a gradual decrease with increasing $NiSO_4$ content. In view of Table 1 and Figure 9, the higher the acidity, the higher the catalytic activity. Good correlations have been found in many cases between the acidity and the catalytic activities of solid acids. For example, the rates of both the catalytic decomposition of cumene and the polymerization of propylene over SiO_2-Al_2O_3 catalysts were found to increase with increasing acid amount at strength $H_0 \leq +3.3$.[40] The catalytic activity of nickel-containing catalysts in ethylene dimerization as well as in butene isomerization is closely correlated with the acidity of the catalyst.[4,9,10,43]

Variation of product composition in ethylene dimerization. It is necessary to confirm that the initial product of ethylene dimerization is 1-butene. The compositions are plotted against the reaction time in Figure 10. In the composition of n-butenes analyzed by gas chromatography, 1-butene was found exclusively at the initial reaction time, and no *cis*- or *trans*-2-butanes were found. However, the amount of 1-butene decreases with the reaction time, while the amount of 2-butenes increases. Therefore, it is obvious that the initially produced 1-butene is also isomerized to 2-butene during the reaction.[4,9] $NiSO_4/Fe_2O_3$ was effective for ethylene dimerization, but Fe_2O_3 without $NiSO_4$ and pure $NiSO_4$ without Fe_2O_3 exhibited absolutely no catalytic activity.

Catalytic activity as a function of acidity. As mentioned above, the active site responsible for dimerization is suggested to consist of a low valent nickel ion and an acid, as observed in the nickel-containing catalyst.[4,30,38] A low-valent nickel, Ni^+, plays the role of an adsorption site for ethylene, while acidic sites are responsible for the formation of reaction intermediates such as ethyl cations.[38] It is known that for ethylene dimerization the variations in catalytic activities are closely correlated to the acidity values of catalyst.[30-47] The acidity values of several samples after evacuation at 400 °C are listed in Table 1 together with their surface areas. In view of Table 1, the catalytic activities substantially run parallel to the acidity values. The catalytic activities of $NiSO_4/Fe_2O_3$ catalysts containing different $NiSO_4$ contents were examined; the results are shown as a function of acidity in Figure 11, where catalysts were evacuated at 500 °C for 1 h before reaction. It is confirmed that the catalytic activity gives a maximum at 20-$NiSO_4/Fe_2O_3$ containing 20 wt % of $NiSO_4$. This seems to be correlated to the specific surface area and to the acidity of the catalysts. The acidity of catalysts calcined at 500 °C was determined by the amount of NH_3 irreversibly adsorbed at 230 °C.[3,4,6,9,48] As shown in Figure 11, the higher the acidity, the higher the catalytic activity. In this way it is demonstrated that the catalytic activity of supported $NiSO_4$ catalysts essentially runs parallel to the acidity. Good correlations have been found in many cases between the acidity and the catalytic activities of solid acids. It has been reported that the catalytic activity of nickel-containing catalysts in ethylene dimerization as well as in butene isomerization are closely correlated with the acidity of the catalysts.[3,4,6,30]

Conclusions

A series of catalysts, $NiSO_4/Fe_2O_3$, was prepared by the

impregnation method using an aqueous solution of nickel sulfate. The addition of nickel sulfate to Fe_2O_3 shifted the phase transition of Fe_2O_3 (from amorphous to hematite) to higher temperatures because of the interaction between nickel sulfate and Fe_2O_3. 20-$NiSO_4/Fe_2O_3$ containing 20 wt % of $NiSO_4$ and calcined at 500 °C exhibited a maximum catalytic activity for ethylene dimerization. $NiSO_4/Fe_2O_3$ catalysts were very effective for ethylene dimerization even at room temperature, but Fe_2O_3 without $NiSO_4$ did not exhibit any catalytic activity at all. The catalytic activity was correlated with the acidity of catalysts measured by the ammonia chemisorption method.

Acknowledgements. This work was supported by 2006 Research Fund of University of Ulsan. We wish to thank Korea Basic Science Institute (Daegu Branch) for the use of their X-ray diffractometer.

References

1. Pae, Y. I.; Lee, S. H.; Sohn, J. R. *Catal. Lett.* **2005**, *99*, 241.
2. Bernardi, F.; Bottoni, A.; Rossi, I. *J. Am. Chem. Soc.* **1998**, *120*, 7770.
3. Sohn, J. R.; Ozaki, A. *J. Catal.* **1979**, *59*, 303.
4. Sohn, J. R.; Ozaki, A. *J. Catal.* **1980**, *61*, 29.
5. Wendt, G.; Fritsch, E.; Schöllner, R.; Siegel, H. Z. *Anorg. Allg. Chem.* **1980**, *467*, 51.
6. Sohn, J. R.; Shin, D. C. *J. Catal.* **1996**, *160*, 314.
7. Berndt, G. F.; Thomson, S. J.; Webb, G. J. *J. Chem. Soc. Faraday Trans.* **1983**, *179*, 195.
8. Herwijnen, T. V.; Doesburg, H. V.; Jong, D. V. *J. Catal.* **1973**, *28*, 391.
9. Sohn, J. R.; Park, W. C.; Kim, H. W. *J. Catal.* **2002**, *209*, 69.
10. Sohn, J. R.; Park, W. C. *Bull. Korean Chem. Soc.* **2000**, *21*, 1063.
11. Urabe, K.; Koga, M.; Izumi, Y. *J. Chem. Soc., Chem. Commun.* **1989**, 807.
12. Wendt, G.; Hentschel, D.; Finster, J.; Schöllner, R. *J. Chem. Soc. Faraday Trans.* **1983**, *179*, 2013.
13. Kimura, K.; Ozaki, A. *J. Catal.* **1964**, *3*, 395.
14. Maruya, K.; Ozaki, A. *Bull. Chem. Soc. Jpn.* **1973**, *46*, 351.
15. Hartmann, M.; Pöppl, A.; Kevan, L. *J. Phys. Chem.* **1996**, *100*, 9906.
16. Elev, I. V.; Shelimov, B. N.; Kazansky, V. B. *J. Catal.* **1984**, *89*, 470.
17. Choo, H.; Kevan, L. *J. Phys. Chem. B* **2001**, *105*, 6353.
18. Tanabe, K.; Misono, M.; Ono, Y.; Hattori, H. *New Solid Acids and Bases*; Kodansha-Elsevier: Tokyo, 1989; p 185.
19. Arata, K.; Hino, M.; Yamagata, N. *Bull. Chem. Soc. Jpn.* **1990**, *63*, 244.
20. Sohn, J. R.; Kim, H. W.; Lim, J. S. *J. Ind. Eng. Chem.* **2006**, *12*, 104.
21. Hino, M.; Arata, K. *Chem. Lett.* **1979**, 1259.
22. Hino, M.; Arata, K. *Chem. Lett.* **1980**, 963.
23. Tanabe, K.; Kayo, A.; Yamaguchi, T. *J. Chem. Soc., Chem. Commun.* **1981**, 602.
24. Kayo, A.; Yamaguchi, T.; Tanabe, K. *J. Catal.* **1983**, *83*, 99.
25. Tanabe, K.; Hattori, H.; Yamaguchi, T.; Yokoyama, S.; Umematsu, J.; Sanada, Y. *Fuel* **1982**, *61*, 389.
26. Hsu, C. Y.; Heimbuch, C. R.; Armes, C. T.; Gates, B. C. *J. Chem. Soc., Chem. Commun.* **1992**, 1645.
27. Cheung, T. K.; Gates, B. C. *J. Catal.* **1997**, *168*, 522.
28. Coelho, M. A.; Resasco, D. E.; Sikabwe, E. C.; White, R. L. *Catal. Lett.* **1995**, *32*, 253.
29. Sohn, J. R.; Lee, S. H. *Appl. Catal. A: Gen.* **2004**, *266*, 89.
30. Sohn, J. R.; Lim, J. S. *Bull. Korean Chem. Soc.* **2005**, *26*, 1029.
31. Sohn, J. R.; Lee, S. G.; Shin, D. C. *Bull. Korean Chem. Soc.* **2006**, *27*, 1623.
32. Sohn, J. R.; Kim, J. G.; Kwon, T. D.; Park, E. H. *Langmuir* **2002**, *18*, 1666.
33. Saur, O.; Bensitel, M. A. B.; Saad, M.; Lavalley, J. C.; Tripp, C. P.; Morrow, B. A. *J. Catal.* **1986**, *99*, 104.
34. Yamaguchi, T. *Appl. Catal.* **1990**, *61*, 25.
35. Morrow, B. A.; McFarlane, R. A.; Lion, M.; Lavalley, J. C. *J. Catal.* **1987**, *107*, 232.
36. Sohn, J. R.; Park, W. C. *Appl. Catal. A: Gen.* **2002**, *230*, 11.
37. Hua, W.; Xia, Y.; Yue, Y.; Gao, Z. *J. Catal.* **2000**, *196*, 104.
38. Sohn, J. R.; Park, W. C. *Appl. Catal. A: Gen.* **2003**, *239*, 269.
39. Siriwardane, R. V.; Poston, J. A. Jr.; Fisher, E. P.; Shen, M. S.; Miltz, A. L. *Appl. Surf. Sci.* **1999**, *152*, 219.
40. Sohn, J. R. *J. Ind. Eng. Chem.* **2004**, *10*, 1.
41. Satsuma, A.; Hattori, A.; Mizutani, K.; Furuta, A.; Miyamoto, A.; Hattori, T.; Murakami, Y. *J. Phys. Chem.* **1988**, *92*, 6052.
42. Sohn, J. R.; Lee, S. H. *Appl. Catal. A: Gen.* **2004**, *266*, 89.
43. Sohn, J. R.; Lee, S. H. *Appl. Catal. A: Gen.* **2007**, *321*, 27.
44. Arata, K. *Adv. Catal.* **1990**, *37*, 165.
45. Yamaguch, T.; Jim, T.; Tanabe, K. J. *Phys. Chem.* **1986**, *90*, 3148.
46. Tanabe, K. *Solid Acids and Bases*; Kodansha, Tokyo, 1970; p 103.
47. Sohn, J. R.; Lim, J. S. *Catal. Today* **2006**, *111*, 403.
48. Sohn, J. R.; Han, J. S. *J. Ind. Eng. Chem.* **2005**, *11*, 439.